Termination of Atrial Fibrillation Using Pulsed Low-Energy Far-Field Stimulation

Flavio H. Fenton, Stefan Luther, Elizabeth M. Cherry, Niels F. Otani, Valentin Krinsky, Alain Pumir, Eberhard Bodenschatz and Robert F. Gilmour, Jr

Circulation published online Jul 27, 2009;
DOI: 10.1161/CIRCULATIONAHA.108.825091
Circulation is published by the American Heart Association. 7272 Greenville Avenue, Dallas, TX 72514
 Print ISSN: 0009-7322. Online ISSN: 1524-4539

Termination of Atrial Fibrillation Using Pulsed Low-Energy Far-Field Stimulation

Flavio H. Fenton, PhD*; Stefan Luther, PhD*; Elizabeth M. Cherry, PhD; Niels F. Otani, PhD; Valentin Krinsky, PhD; Alain Pumir, PhD; Eberhard Bodenschatz, PhD; Robert F. Gilmour, Jr, PhD

Background—Electrically based therapies for terminating atrial fibrillation (AF) currently fall into 2 categories: antitachycardia pacing and cardioversion. Antitachycardia pacing uses low-intensity pacing stimuli delivered via a single electrode and is effective for terminating slower tachycardias but is less effective for treating AF. In contrast, cardioversion uses a single high-voltage shock to terminate AF reliably, but the voltages required produce undesirable side effects, including tissue damage and pain. We propose a new method to terminate AF called *far-field antifibrillation pacing*, which delivers a short train of low-intensity electric pulses at the frequency of antitachycardia pacing but from field electrodes. Prior theoretical work has suggested that this approach can create a large number of activation sites ("virtual" electrodes) that emit propagating waves within the tissue without implanting physical electrodes and thereby may be more effective than point-source stimulation.

Methods and Results—Using optical mapping in isolated perfused canine atrial preparations, we show that a series of pulses at low field strength (0.9 to 1.4 V/cm) is sufficient to entrain and subsequently extinguish AF with a success rate of 93% (69 of 74 trials in 8 preparations). We further demonstrate that the mechanism behind far-field antifibrillation pacing success is the generation of wave emission sites within the tissue by the applied electric field, which entrains the tissue as the field is pulsed.

Conclusions—AF in our model can be terminated by far-field antifibrillation pacing with only 13% of the energy required for cardioversion. Further studies are needed to determine whether this marked reduction in energy can increase the effectiveness and safety of terminating atrial tachyarrhythmias clinically. **(*Circulation*. 2009;120:467-476.)**

Key Words: arrhythmia ■ atrium ■ cardioversion ■ fibrillation ■ mapping

Atrial fibrillation (AF) is the most common sustained cardiac arrhythmia worldwide,[1] affecting >2.2 million people in the United States alone.[2] Complications associated with chronic AF include increased risk for both thromboembolism and stroke.[2] Left untreated, paroxysmal AF often progresses to permanent AF, which is resistant to therapy.[3] Although underlying anatomic or pathophysiological factors may fuel this progression,[3] AF itself may lead to its own perpetuation through electric, structural, and metabolic remodeling of atrial tissue. The realization that AF begets AF[4] has led to management strategies that are designed to avoid the progression of AF by reducing the frequency and duration of AF episodes.

Clinical Perspective on p 476

One such strategy, cardioversion, attempts to reset all electric activity in the atria and requires the use of large (>5 V/cm) electric field gradients.[5–7] These high energies cause pain and trauma for the patient, damage the myocardium, and reduce battery life in implanted devices.[8] Another strategy, antitachycardia pacing (ATP), seeks to avoid the development of permanent AF by suppressing paroxysmal AF. ATP consists of a train of 8 to 10 low-energy stimuli delivered as a pacing ramp or burst at 50 Hz via a single pacing electrode.[9] ATP is effective in treating spontaneous atrial tachyarrhythmias, especially slower tachycardias,[9–10] but it is not very effective for converting AF.[9,11,12]

To overcome the limitations of ATP and cardioversion, we propose a new technique that employs a series of low-amplitude pulsed electric fields to overdrive AF and thereby terminate it, a strategy suggested by previous experimental studies with the use of physically implanted electrodes.[13,14] The technique, which we call *far-field antifibrillation pacing*

Received September 29, 2008; accepted June 5, 2009.

From the Department of Biomedical Sciences (F.H.F., S.L., E.M.C., N.F.O., R.F.G.) and Laboratory of Solid State Physics and Department of Mechanical and Aerospace Engineering (E.B.), Cornell University, Ithaca, NY; Max Planck Institute for Dynamics and Self-Organization, Göttingen, Germany (S.L., E.B.); Institute Non Lineáire de Nice, Valbonne, France (V.K.); and Laboratoire de Physique, Ecole Normale Supérieure de Lyon, Lyon, France (A.P.).

*Drs Fenton and Luther contributed equally to this work.

The online-only Data Supplement is available with this article at http://circ.ahajournals.org/cgi/content/full/CIRCULATIONAHA.108.825091/DC1.

Correspondence to Flavio H. Fenton, PhD, Department of Biomedical Sciences, T7 012C Veterinary Research Tower, College of Veterinary Medicine, Cornell University, Ithaca, NY 14853 (E-mail fhf3@cornell.edu), or Stefan Luther, PhD, Max Planck Institute for Dynamics and Self-Organization, Am Fassberg 17, D-37077, Göttingen, Germany (E-mail stefan.luther@ds.mpg.de).

Circulation **is available at http://circ.ahajournals.org** **DOI: 10.1161/CIRCULATIONAHA.108.825091**

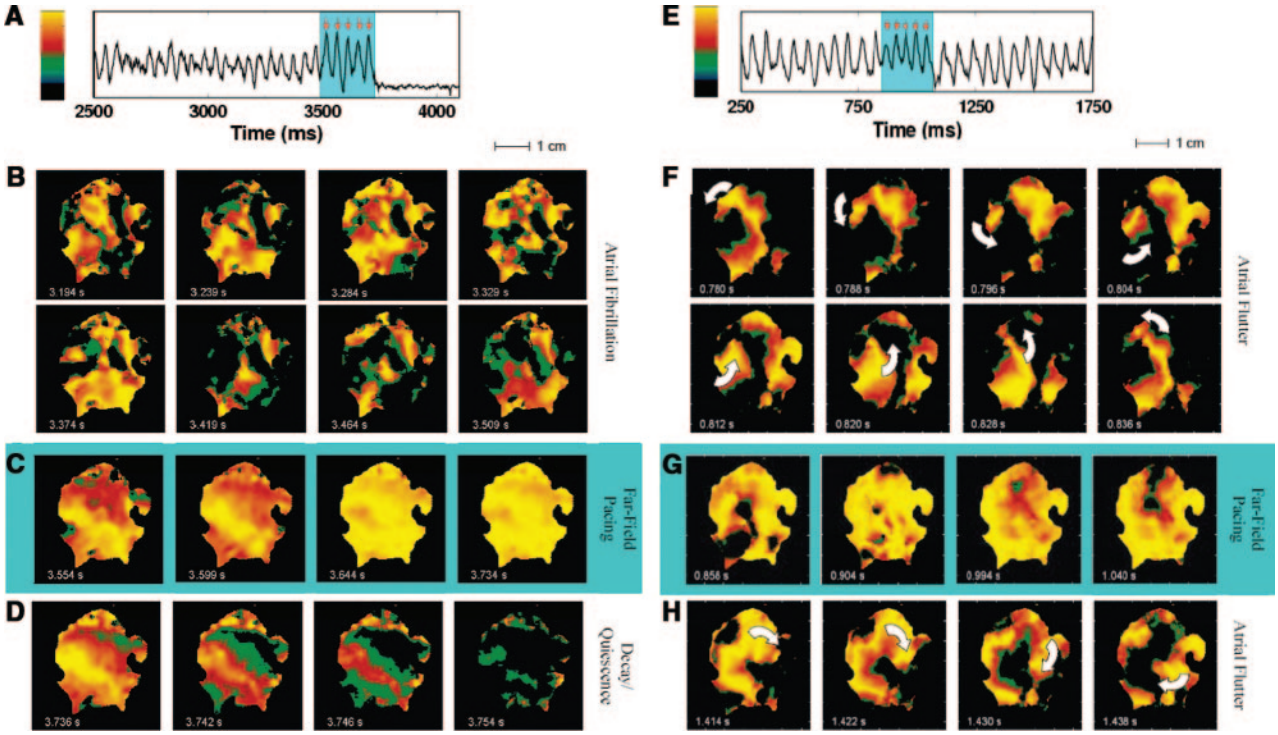

Figure 1. Successful and unsuccessful termination of AF. A, Optical signal from 1 pixel during AF showing successful defibrillation after delivery of 5 far-field pulses of 1.4 V/cm at a cycle length of 45 ms (red arrows). B, Optical signal during fibrillation; color represents voltage (see color bar in A). Frames are 45 ms apart in time and show the complex wave patterns during fibrillation. C, Effects of shocks 1, 2, 3, and 5 (left to right), with the first 2 panels showing partial capture and the last 2 showing global capture. D, Evolution to full repolarization and quiescence after shock 5. E, Optical signal from 1 pixel during atrial flutter showing unsuccessful defibrillation after 5 field pulses of 0.9 V/cm at a cycle length of 45 ms (red arrows). F, Optical signal showing a spiral wave rotating counterclockwise before the shocks. G, Partial capture by shocks 1, 2, 4, and 5 (left to right). H, Shock-induced conversion of the original spiral wave into a spiral wave rotating clockwise. Throughout, light blue shading indicates time during applied shocks.

(FF-AFP), takes advantage of the fact that after an electric field pulse, virtual electrodes may arise at interfaces separating regions with different conductivities.[15] These sites may be macroscopic, such as blood vessels or ischemic regions, or smaller-scale discontinuities, including areas of fibrosis or abrupt changes in fiber direction.[16–21] Virtual electrodes may become a secondary source (ie, a site of wave emission), depending on the extent of the conductivity discontinuity and the electric field strength.

Here we use a combination of computer simulations and experiments in isolated perfused canine cardiac preparations to demonstrate that FF-AFP can terminate AF with a high success rate, even at low energies. We further show that the method is successful because the electric field creates many activation sites in the vicinity of endogenous conductivity discontinuities,[16–21] which in turn produce propagating waves, as predicted by previous studies.[22–25] Given that the virtual electrodes created by field stimulation substitute for multiple physically implanted electrodes, this approach promises to provide a means of suppressing atrial tachyarrhythmias less invasively and with less physical and psychological trauma than with currently available therapy.

Methods

Tissue Preparation

Studies were performed with the use of hearts obtained from adult mongrel dogs of either sex weighing 10 to 30 kg. The experimental procedures were approved by the Institutional Animal Care and Use Committee of the Center for Animal Resources and Education at Cornell University. The dogs were anesthetized with Fatal-Plus (390 mg/mL pentobarbital sodium; Vortex Pharmaceuticals; 86 mg/kg IV), and their hearts were excised rapidly. The right coronary artery was cannulated with polyethylene tubing, and the right atrial myocardium and ventricular myocardium perfused by that artery were excised and suspended in a heated (37°C) transparent tissue chamber where they were both perfused and superfused with normal Tyrode solution. After 15 to 30 minutes of equilibration, the preparation was stained with the voltage-sensitive dye Di-4-ANEPPS (10 μmol/L bolus). Blebbistatin (10 μmol/L constant infusion over 30 to 40 minutes) was added to prevent motion artifact.[26] Arrhythmias were induced by applying acetylcholine (1 to 4 μmol/L) and initiating burst pacing with a frequency of 40 Hz and amplitude of 8 V.[27] Different concentrations of acetylcholine produced a range of arrhythmias having dominant periods between 30 and 65 ms, which provided an opportunity to create arrhythmias that simulated atrial tachycardia, atrial flutter, and AF in an intact heart. If shocks were not applied, AF was persistent (maximum time tracked was 2 hours). Field stimulating electrodes consisted of 1-cm×5-cm^2 platinum plates embedded in epoxy and were placed on either side of the preparation 10 cm apart. Pacing and far-field stimuli consisted of rectangular pulses delivered, respectively, with a stimulator and stimulus isolator (World Precision Instruments) and a function generator (Agilent 33220A) coupled to a power amplifier (Kepco BOB 100 to 4 mol/L) capable of delivering field strengths from 0.01 to 4.6 V/cm at cycle lengths as short as 30 ms. The field strength between the electrodes was measured with the use of 2 Teflon-coated silver wires 5 to 7 cm apart and immersed in the bath. Tissue cryoablation was performed by pressing a metal circle or rectangle previously frozen in liquid nitrogen against the tissue surface for ≈1 minute.

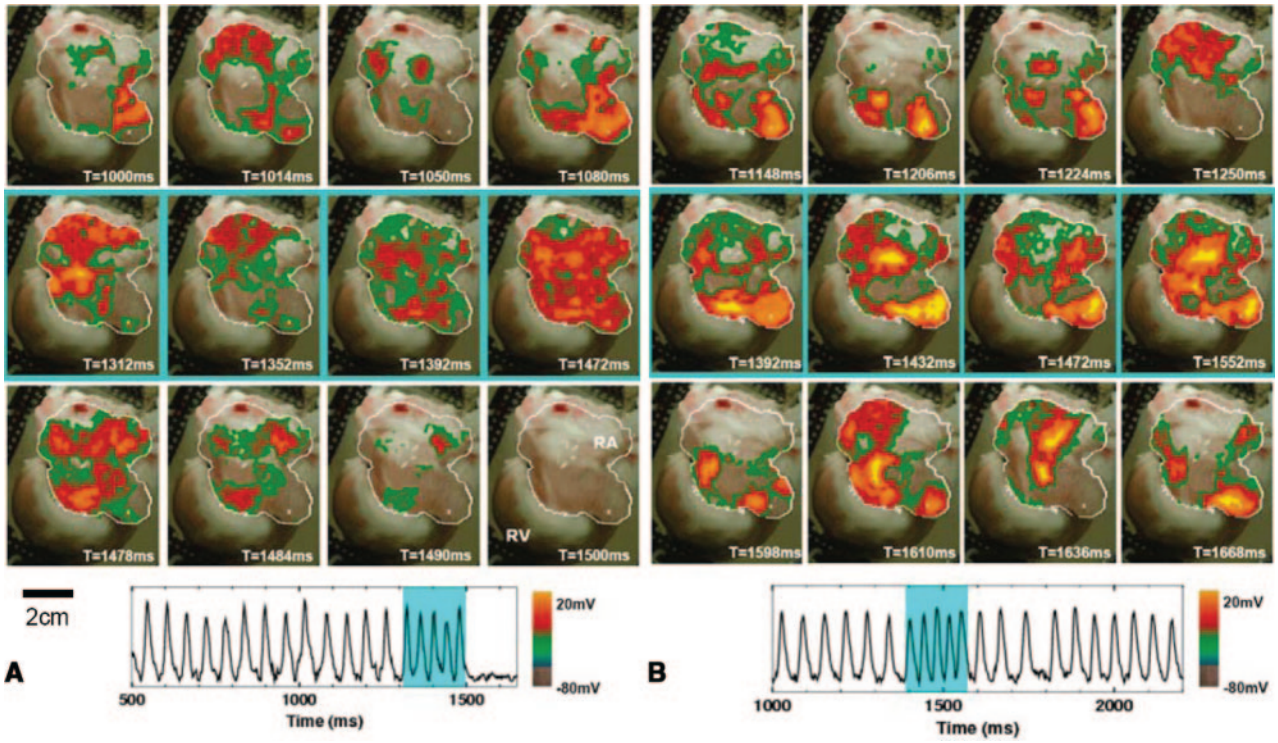

Figure 2. Successful and unsuccessful termination of AF. A, Successful termination. Top row, AF (dominant period=59 ms) preceding FF-AFP. Middle row, Shocks 1, 2, 3, and 5 in a series of 5 electric field pulses 40 ms apart (1.63 V/cm, 5-ms duration). Tissue area captured progressively increases. Bottom row, Return to quiescence after the last pulse. Tracing shows optical signal from 1 pixel (white cross in the above panels, lower right) before, during, and after FF-AFP. Light blue shading indicates time during applied shocks. B, Unsuccessful termination. Top row, AF (dominant period=60 ms) preceding FF-AFP. Middle row, Shocks 1, 3, 4, and 5 in a series of 5 electric field pulses 40 ms apart (1.40 V/cm, 5-ms duration). Not enough tissue is captured by the last pulse to terminate the arrhythmia. Bottom row, Return to AF. Tracing shows optical signal from 1 pixel (white cross in the above panels, lower right) before, during, and after FF-AFP. Light blue shading indicates time during applied shocks.

Optical Mapping

Excitation light was produced by 16 high-performance light-emitting diodes (Luxeon III star, LXHL-FM3C, wavelength 530±20 nm) driven by a low-noise constant-current source. The illumination efficiency was significantly enhanced by collimator lenses (Luxeon, LXHL-NX05). The fluorescence emission light was collected by a Navitar lens (DO-2595, focal length 25 mm, F/# 0.95), passed through a long-pass filter (<610 nm), and imaged by a 128×128 back-illuminated electron-multiplied charge-coupled device array (Photometrics Cascade 128+). The signal was digitized with a 16-bit analog/digital converter at a frame rate of 511 Hz (full frame, 128×128 pixels). The peripheral component interconnect interface provided high-bandwidth uninterrupted data transfer to the host computer. The instantaneous dominant frequency of an arrhythmia was obtained in real time by calculating the fast Fourier transform of the signal recorded from 1 pixel in the center of the preparation in real time.

FF-AFP and Cardioversion Protocols

For the FF-AFP experiments, a sequence of either 5 or 10 pulses was applied with a 5-ms pulse duration and a cycle length 5 to 10 ms below the dominant cycle length of the arrhythmia. The electric activation of the atria was recorded as described above, and the optical activation pattern was then characterized and its dependency on stimulation energy calculated. A series of recordings was made in each experiment, with each recording lasting up to 15 seconds in duration. Field strength was varied and applied from the threshold level of activation (0.25 V/cm), as determined before arrhythmia induction, until arrhythmia termination was achieved or the maximal deliverable field strength was reached (≈4.6 V/cm).

Computer Simulations

Computer simulations were performed with a bidomain model subject to no-flux boundary conditions, with irregular boundaries handled with the use of either a finite-volume formulation or a phase-field method.[28] Forward Euler with GMRes was used to solve the bidomain equations, as follows:

$$C_m\partial(\boldsymbol{V_i}-\boldsymbol{V_e})/\partial t=\nabla D_i\nabla(\boldsymbol{V_i}-\boldsymbol{V_e})-\boldsymbol{J_{ion}}$$
$$C_m\partial(\boldsymbol{V_i}-\boldsymbol{V_e})/\partial t=-\nabla D_e\nabla(\boldsymbol{V_i}-\boldsymbol{V_e})+\boldsymbol{J_{ion}} \quad (1)$$

where V_i and V_e are the intracellular and extracellular potentials, the membrane potential is given by $V_m=V_i-V_e$, and the intracellular and extracellular diffusions are given by D_i and D_e. The membrane dynamics is given by the ionic current density J_{ion}. Two realistic ionic models were used.[29,30] In some cases, the insulating plaque that typically forms between myocardial fibers in older hearts[31] was modeled by randomly removing gap junctions along short lines (average length 625 μm) oriented along the fiber direction (average spacing 2.5 mm). Atrial simulations included the acetylcholine-activated K^+ current.[32] Less intense computations were performed on a desktop computer, whereas larger computations were performed on a 4136-processor Cray XT3 MPP machine at the Pittsburgh Supercomputing Center.

Statistical Analysis

Data are expressed as mean±SE. Statistical significance was determined by comparing the log of the ratio of the FF-AFP energy requirement and the standard defibrillation energy requirement with the use of restricted maximum likelihood estimates for a random-effects model implemented in the JMP statistical package. Be-

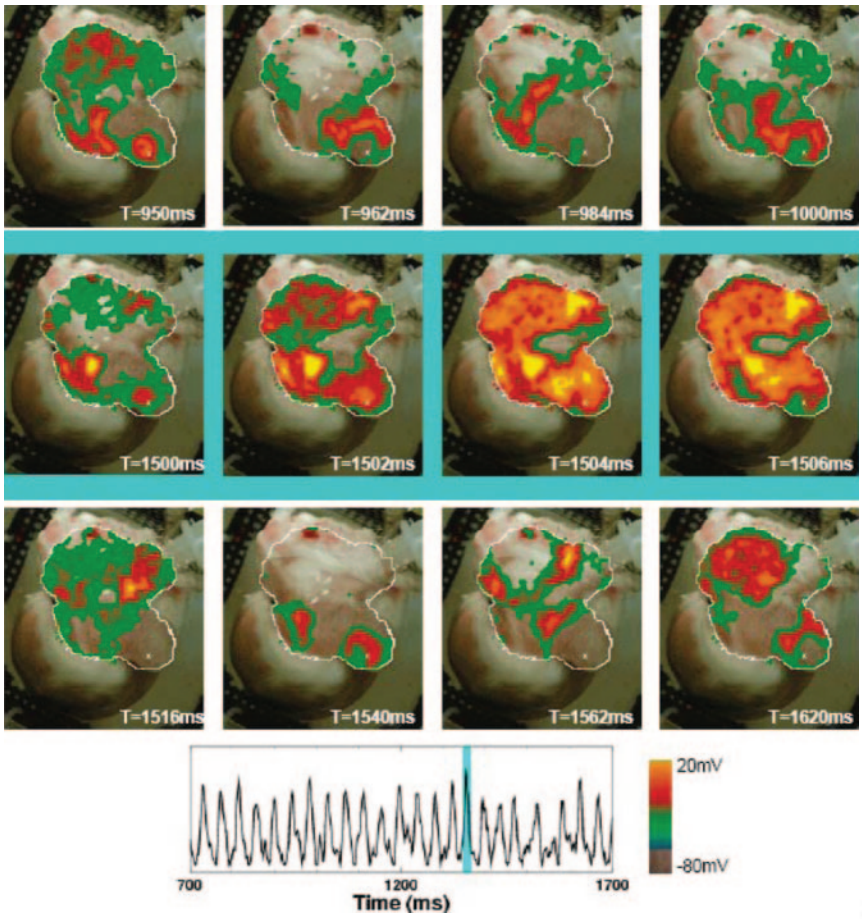

Figure 3. Unsuccessful termination of AF with use of a single high-voltage pulse. Top row shows AF preceding application of a single electric field pulse (4.67 V/cm, 5-ms duration), which fails to capture the entire tissue (middle row). Bottom row shows the return to arrhythmia after the pulse. Tracing shows optical signal from 1 pixel (white cross in the above panels, lower right) before, during, and after FF-AFP. Light blue shading indicates time during applied shock (2 μmol/L acetylcholine).

cause multiple trials were performed in individual preparations, a random-effects model was used to account for the correlation of observations from the same preparation. $P<0.05$ was considered significant.

Results

Termination of Atrial Arrhythmias With FF-AFP

Prior theoretical work[24] has suggested that low-energy cardioversion may be possible by applying a pulsed electric field. To test this hypothesis, we induced sustained arrhythmias in excised canine atrial tissue preparations, applied a pulsed electric field, and used optical mapping to record the electric activity before and after delivery of the field. Figure 1A through 1D and the online-only Data Supplement Movie I show an example of successful AF termination via FF-AFP. Optical signals for the mapped atrium, along with the signal recorded from 1 pixel during AF, are shown, with the light blue shaded regions indicating the time during which far-field pulses of 1.4 V/cm were delivered at a cycle length of 45 ms. Complex nonrepeating electric wave patterns that characterize AF were seen before application of FF-AFP shocks (Figure 1B). The initial FF-AFP shock entrained only part of the tissue (first panel in Figure 1C), whereas subsequent shocks entrained progressively more tissue until the entire mapped area was activated by the last shock (last panel in Figure 1C). After delivery of 5 shocks, the arrhythmia terminated, and full repolarization and quiescence ensued (Figure 1D). An additional example of successful conversion of AF in a different preparation can be seen in Figure 2A and online-only Data Supplement Movie II. In this case, successful termination occurred after the delivery of 5 far-field pulses of 1.63 V/cm at a cycle length of 40 ms.

If the electric field strength was too low, an insufficient number of activation sites were recruited, and only partial entrainment occurred, resulting in an unsuccessful defibrillation attempt, as shown in Figure 1E through 1H and online-only Data Supplement Movie III. Although the lower field strength of 0.9 V/cm altered activation patterns during AF and even changed the chirality of the reentry (compare Figure 1F and Figure 1H), it did not fully entrain the tissue. Consequently, the arrhythmia persisted. Figure 2B and online-only Data Supplement Movie IV show another unsuccessful defibrillation attempt with a field strength of 1.40 V/cm in the same preparation as Figure 2A.

FF-AFP was effective over a broad range of dominant arrhythmia periods (30 to 65 ms) generated with different concentrations of acetylcholine (1 to 4 μmol/L), as illustrated in online-only Data Supplement Figure I, which shows optical signals from 1 pixel for 6 different arrhythmia episodes successfully terminated with the use of FF-AFP (field strength 1.40 V/cm). In a total of 74 trials in 8 preparations, FF-AFP terminated 69 episodes of AF, resulting in a 93% success rate. Of those 69 episodes, 45 were terminated with a single series of 5 pulses, and 24 required additional attempts (up to a maximum of 4). Each of the preparations used for these studies contained a large

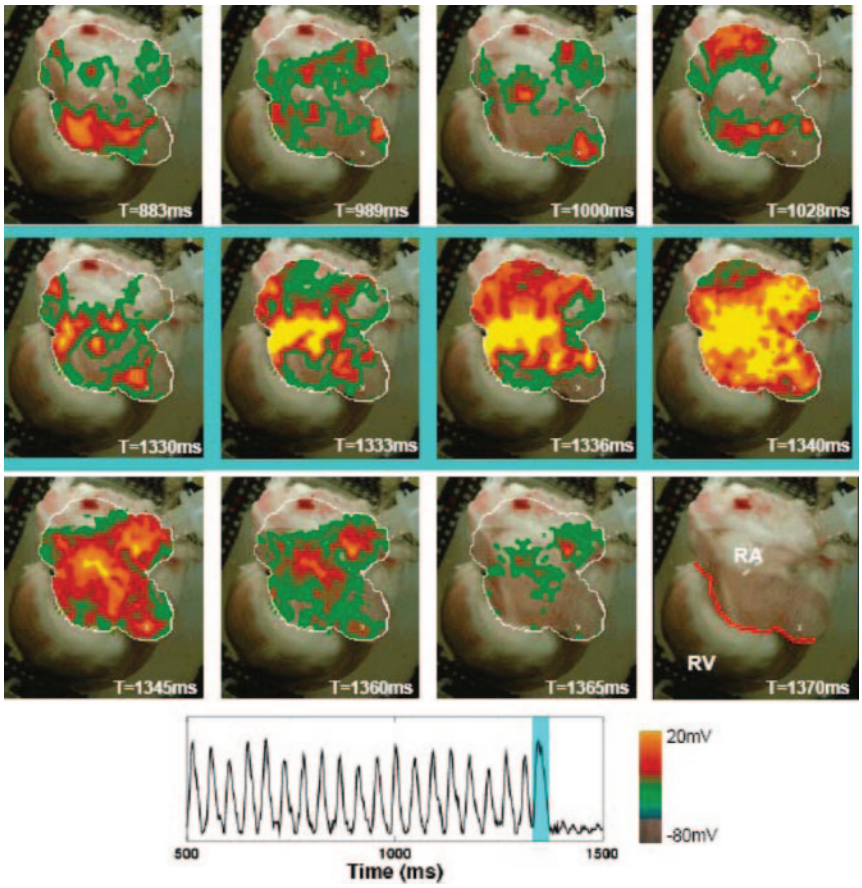

Figure 4. Successful termination of AF with use of a single high-voltage pulse. Top row shows AF preceding application of a single electric field pulse (3.73 V/cm, 10-ms duration), which successfully captures the entire tissue (middle row). Bottom row shows quiescence after the pulse. Tracing shows optical signal from 1 pixel (white cross in the above panels, lower right) before, during, and after FF-AFP. The last panel indicates tissue geometry, with the red line separating the right atrium from the right ventricle. Light blue shading indicates time during applied shock. Same preparation was used as in (2 μmol/L acetylcholine).

enough portion of the right ventricle to support ventricular fibrillation (see online-only Data Supplement Figure II and Movie V), but in no case did FF-AFP induce ventricular fibrillation.

Energy Reduction Achieved by Terminating Atrial Arrhythmias With FF-AFP Compared With a Single Shock

For comparison, in 12 trials in 4 preparations, the electric field strengths required to terminate AF with FF-AFP were compared with those required to terminate AF with a single shock (akin to standard cardioversion). Figure 3 and online-only Data Supplement Movie VI show an example of an episode of AF that could not be defibrillated by a single strong shock of 4.67 V/cm applied for 5 ms, comparable to the 5 V/cm typically required for cardioversion.[5] To terminate AF in this preparation with a single shock, it was necessary to apply a minimum electric field strength of 3.73 V/cm for 10 ms, with a corresponding energy of 4.26 J, as shown in Figure 4 and online-only Data Supplement Movie VII. In comparison, each FF-AFP shock in the successful defibrillation shown for the same preparation in Figure 4 required only 0.4 J, a reduction in energy of 91%. Overall, the average energy required for defibrillation with FF-AFP was 12.4±1.9% of that required for a single shock ($P<0.002$).

FF-AFP Mechanism: Generation of Activation Sites Within the Tissue

We hypothesized that FF-AFP terminates AF by synchronizing tissue activation. Synchronization occurs because the pulsed electric fields create virtual electrodes at conductivity discontinuities, which results in the activation of increasingly larger regions of tissue with successive pulses.

To test this idea, we first determined the response to a single electric field pulse in quiescent tissue. Figure 5A illustrates schematically how an activation site develops on application of an electric field in a 1-dimensional circuit representation of cardiac tissue containing a generic conductivity discontinuity between myocardium and an inexcitable obstacle. Three separate interfaces between excitable and inexcitable regions are included: the single obstacle and the 2 tissue edges. When an electric field is applied, current flows out from the positive electrode through the extracellular medium and enters the tissue at the tissue edge and subsequently exits at the boundary of the inexcitable region. Similarly, on the other side of the inexcitable region, current reenters the tissue at the boundary and exits at the tissue edge. In quiescent tissue, this current produces depolarization (hyperpolarization), shown in red (blue), in the conducting region along all interface boundaries where the excitable tissue is closer to the positive (negative) electrode. The resulting virtual electrodes[16–23] alter electric activity in the tissue without the presence of a physical electrode. If the depolarized region reaches the threshold for excitation, it can initiate propagating waves, thereby serving as an activation site, also known as a secondary source[15] (where the primary source refers to the applied electric field).

This mechanism of virtual electrode generation during field stimulation is illustrated in Figure 5B, which shows the

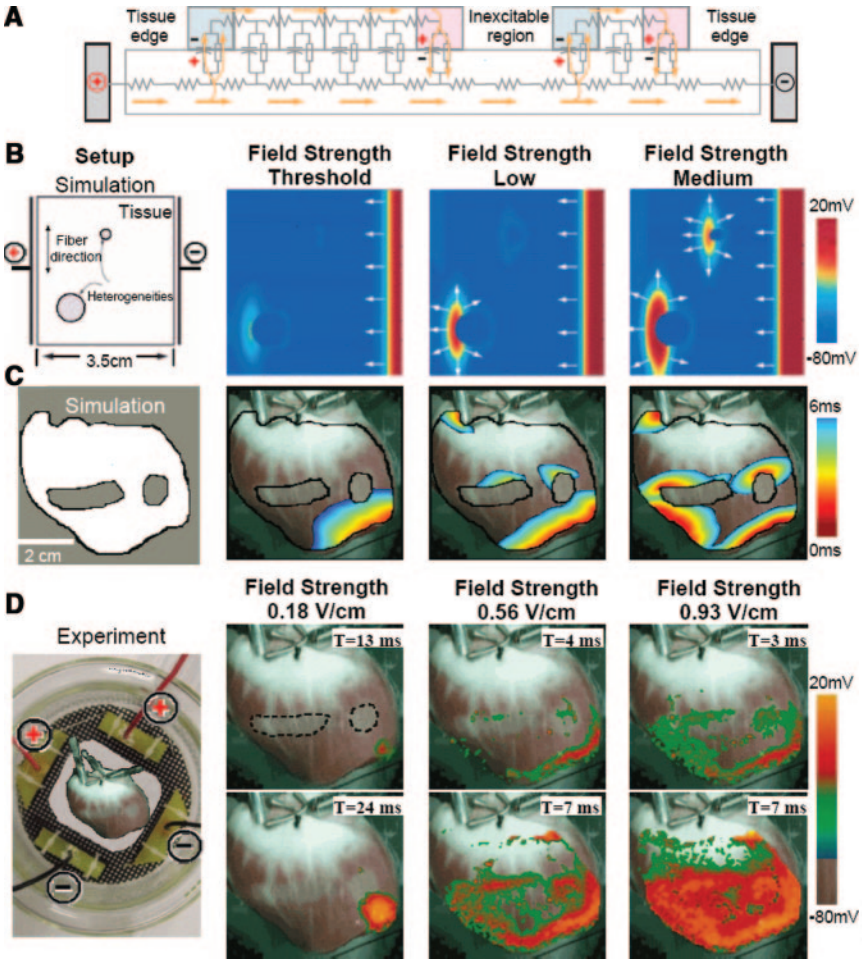

Figure 5. Mechanism of activation site formation. A, Schematic circuit representation of cardiac tissue with an inexcitable obstacle with the bidomain model. Current injected by the positive electrode produces regions of hyperpolarization (blue) and depolarization (red). B, Idealized simulated cardiac tissue with conductivity discontinuities created by 2 inexcitable obstacles. With increasing field strengths, first the tissue edge, then a single conductivity discontinuity, and finally both conductivity discontinuities are excited. Spatial resolution is 250 μm. C, Realistic simulated cardiac tissue with 2 inexcitable obstacles. As in B, increasing the field strength recruits more conductivity discontinuities as virtual electrodes. Spatial resolution is 100 μm. D, Experimental preparation with 2 inexcitable obstacles created by cryoablation shown with a dotted line (geometry as in C). Increased field strengths progressively activate more tissue.

different activation patterns associated with 2 inexcitable circular obstacles in idealized simulated atrial tissue as the electric field strength is increased. The activating shock was delivered by injecting current from the positive electrode (left), which passed through the tissue and exited at the negative electrode (right). At the lowest field strength, only the tissue edge (which constitutes a large conductivity discontinuity) became an activation site. As the electric field strength was increased, tissue near the boundary of the larger obstacle was activated. With a further increase in the field strength, tissue near the boundary of the smaller obstacle was activated as well. Although the entire right edge of the tissue was depolarized, it was the tissue abutting not the right but the left edges of the obstacles that was depolarized, in accordance with Figure 5A.

A similar pattern was observed in the more anatomically realistic setting of Figure 5C and 5D. In this case, 2 regions of an arterially perfused canine ventricular preparation were subjected to cryoablation to create marked conductivity discontinuities. In Figure 5C, a computer simulation of the effects of field stimulation in this setting was conducted with the use of a 2-dimensional ventricular slice digitized from this experimental preparation. As in Figure 5B, at the lowest electric field strength, only the tissue edge closest to the negative electrode was activated. As the field strength was increased, additional activations originated from the edges of the conductivity discontinuities closer to the positive electrode. The same effects were seen in the actual experimental setting in Figure 5D and online-only Data Supplement Movies VIII through XII. As in Figure 5B and 5C, the lowest field strength (0.18 V/cm; Movie VIII) activated only the tissue edge closest to the negative electrode. At a field strength of 0.56 V/cm (Movie X), not only was a larger area of activation produced at the lower edge of the preparation, but activations also were initiated near the edges of the cryoablated regions closer to the positive electrode, as in the simulations. However, unlike the 2-dimensional simulations, in 3-dimensional tissue, activations eventually were seen within the cryoablated regions as well, most likely because the cryoablated areas were not completely transmural. Consequently, tissue below the surface, which was still viable, produced an optical signal.[33] At a field strength of 0.93 V/cm (Movie XII), more tissue around the conductivity discontinuities and at the tissue edges was activated, and optical signals from the cryoablated areas were even more pronounced.

Figure 6 shows simulated atrial tissue simulations where collagenous septa and gap junction conductivity discontinuities were incorporated to represent the insulating plaques that typically form between fibers in older hearts.[31] Figure 6B demonstrates how in this setting the number of activation sites produced by the conductivity discontinuities increased as the field strength was increased from 0.8 to 1.14 V/cm. In

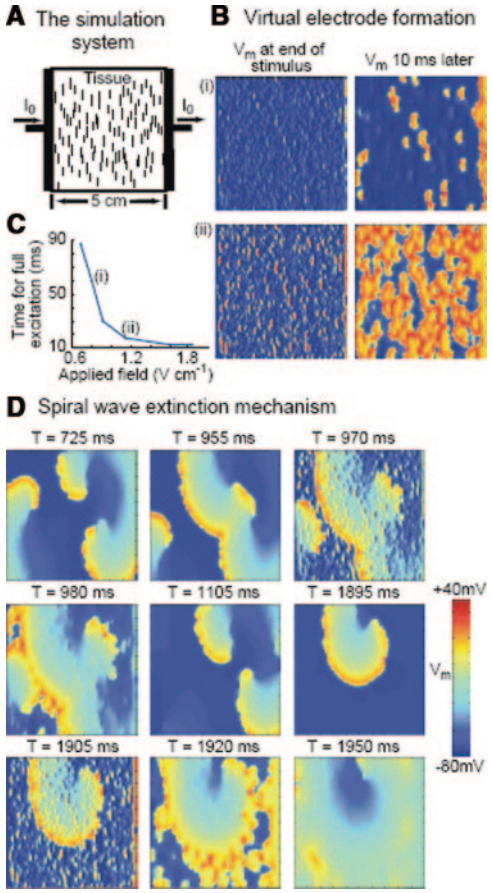

Figure 6. Simulation of virtual electrode formation and termination of reentry in tissue with multiple small conductivity discontinuities. A, Tissue setup schematic. Pacing stimuli are delivered to a square sheet of cardiac tissue by injecting current from the left planar electrode. Collagenous septa (short vertical lines), randomly distributed throughout the tissue, serve as conductivity discontinuities around which induced activations form in response to the applied stimuli. Septa sizes are increased 10 times, and only 1 of every 32 is shown for clarity. Spatial resolution is 250 μm. B, Membrane potential V_m induced in the tissue by field strengths of (i) 0.8 V/cm and (ii) 1.14 V/cm (5 ms, square wave pulse). C, Time required for a single applied stimulus of various field strengths to depolarize the entire tissue from the resting state. D, Termination of reentry by 8 low-voltage shocks at a cycle length corresponding to the spiral wave period. Membrane potential is shown before and after shocks 3 and 8 (S3 and S8, delivered at T=970 ms and T=1905 ms, respectively).

addition, the time required to depolarize the entire tissue decreased with increasing field strength, as shown in Figure 6C for simulated tissue and in Figure 7 for actual atrial tissue.

Unlike in the experimental preparations, in which it was not technically feasible to detect virtual electrode formation during FF-AFP, in the computer simulations it was clear, as shown in Figure 6D and online-only Data Supplement Movie XIII, that FF-AFP generated multiple activation sites at conductivity discontinuities, thereby progressively entraining the entire tissue and terminating the arrhythmia with repeated pulse application. In this case, 3 reentrant waves were terminated after 8 successive monophasic shocks of 5-ms duration at a cycle length matching the spiral wave period.

Discussion

We have demonstrated a new method to terminate fast atrial tachycardias and AF. In this method, electrodes located at a small distance from the heart deliver a train of low-voltage shocks at a rapid rate. Our data are consistent with the idea that during the low-energy shocks, small intrinsic conductivity discontinuities behave as internal "virtual" electrodes.[16–23] The virtual electrodes serve as activation sites (or secondary sources) if the field strength depolarizes the tissue beyond the excitation threshold.[15,16] At very low field strengths, only a single virtual pacing site may be created, whereas at slightly higher field strengths, many more activation sites arise, and the time required to excite a given myocardial preparation decreases[16] (Figure 7F). The more virtual electrodes that are recruited during FF-AFP, the easier it is to entrain the entire tissue and to terminate an arrhythmia.

In a previous study, Ripplinger et al[25] demonstrated that a precisely timed low-voltage electric field could detach a pinned reentrant wave and move it to a boundary for extinction. Although this method is likely to be effective for terminating an arrhythmia arising from a single reentrant source, multiple stimuli applied at numerous sites are required to terminate fibrillation by this phase-coupled approach.[14] As in the Ripplinger et al[25] study, FF-AFP uses an electric field to create activation at a conductivity discontinuity, but the timing of the introduction of the field is not critical in that the objective is not to unpin waves and move them to a boundary but rather to entrain progressively larger regions of tissue. Consequently, FF-AFP is capable of terminating multiple anatomic and functional reentries simultaneously, without moving them to boundaries (see online-only Data Supplement Figure III and Movie XIV), and may therefore be a useful approach for terminating polymorphic tachycardias and fibrillation.

The FF-AFP technique represents an innovative approach to the treatment of AF. Pharmacological therapy is not always successful in terminating atrial arrhythmias or in preventing them from recurring with increasing frequency.[3] Other forms of electric intervention also have a number of limitations. Catheter ablation approaches, for example, although successful in some patient populations,[34] have not been shown to be effective for a broad range of patients.[3] Because of its restriction to a single site, ATP requires a frequency fast enough to extinguish, rather than simply entrain, reentrant waves[10] because the electrode may lie outside the core of the reentrant wave(s). These rapid rates can increase the likelihood of inducing AF.[35] Cardioversion with implantable cardioverter-defibrillators successfully terminates 90% of paroxysmal AF and 75% of persistent AF with biphasic shocks (≈3 ms/3 ms) with mean threshold energies of 7 J.[7,36,37] However, such high-energy shocks produce considerable discomfort in patients[38,39] and damage the myocardium.[40]

Our findings show that FF-AFP has many of the advantages of ATP and cardioversion and fewer of the drawbacks. Specifically, it duplicates the significant success rate of cardioversion (93% in our in vitro experiments) while avoiding damaging high-energy shocks. Moreover, FF-AFP is unique in that it is not simply a modification of either ATP or

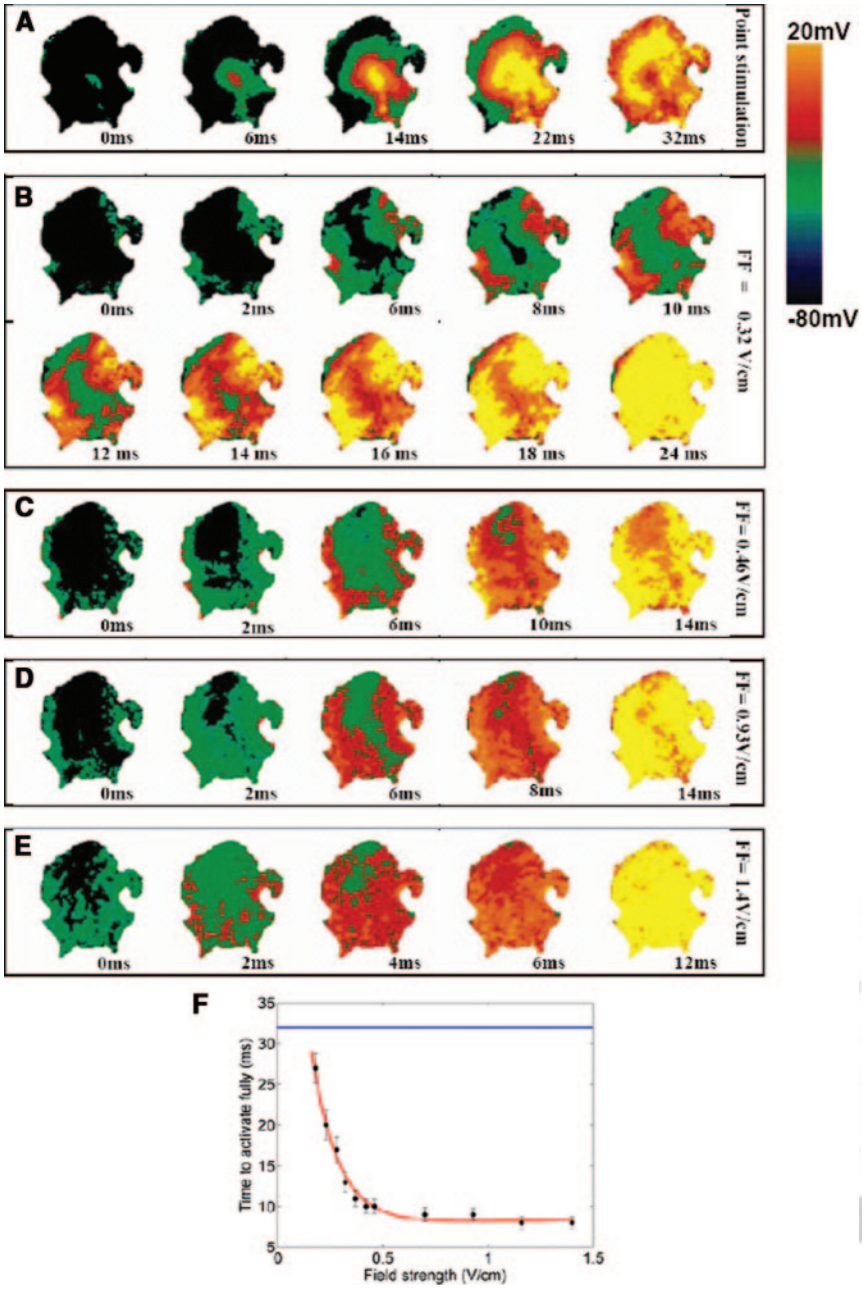

Figure 7. Recruitment of activation sites as a function of field strength in atrial tissue. A, Propagation induced by stimulation with a point electrode. B through E, Activation of tissue by field stimulation at field strengths of 0.32, 0.46, 0.93, and 1.4 V/cm. As field strength is increased, more virtual electrodes are recruited, resulting in more rapid depolarization of the entire tissue. F, Time to full activation of the tissue as a function of electric field strength. Blue line represents time to full activation from a point stimulus.

cardioversion. It relies on low-strength electric fields to induce activations at conductivity discontinuities throughout the tissue. These activation sites have an increased likelihood of generating an excitation that will affect reentrant waves or, more specifically, the excitable gaps between waves, with more nearly synchronous timing. As a result, the excitable gaps are filled almost simultaneously and completely, and because the tissue is fully captured at the FF-AFP pacing cycle length, rotating waves are terminated. With the extinction of reentry, normal sinus rhythm can resume.

In addition to discontinuities in conductivity, dynamical heterogeneities arising from dispersion of repolarization during fibrillation potentially could act as virtual electrodes, especially along activation wavefronts, where the voltage gradients are steepest. However, our computer modeling studies indicate that the effects of electric fields on these dynamical discontinuities during fibrillation are much smaller than those on static conductivity discontinuities (as shown in online-only Data Supplement Figure IV).

The energy needed for successful defibrillation with the use of FF-AFP ranged between 0.074 and 0.81 J, with an average of 0.24 J, which is below the energy at which sedation is necessary (0.5 to 1 J).[38,39] Although the average energy for termination by FF-AFP in our in vitro model is below the pain threshold (0.4 J),[41] the number of FF-AFP shocks could affect pain perception, in that a series of shocks seems more painful than 1 shock, and subsequent shocks subjectively feel stronger even when they are less strong than previous shocks.[7] Nevertheless, it is expected that the use of biphasic, truncated, and other waveforms, instead of the monophasic waveforms used in this study, together with optimized geometry and placement of electrodes[37] will fur-

ther decrease the required FF-AFP energies, possibly to levels below the threshold for pain perception. For instance, biphasic cardioversion shocks with an 80% success rate require less than one third the energy needed to achieve a similar success rate with the use of monophasic shocks.[6] Additionally, FF-AFP may be more effective in older patients and patients with fibrosis or scarring because of the higher incidence of conductivity discontinuities these patients are likely to possess,[31] therefore potentially increasing the number of virtual electrodes recruited and further reducing the energy required for successful cardioversion. Addressing these issues and future clinical relevance will require further studies of the efficacy of FF-AFP in vivo.

Acknowledgments

We thank M.W. Enyeart and D. Raskolnikov for technical assistance and Giles J. Hooker for statistical consultation.

Sources of Funding

This work was supported in part by National Institutes of Health grants HL075515-S03 and HL075515-S04 (Dr Fenton), HL075515 (Dr Gilmour), and HL073644 (Drs Gilmore and Bodenschatz); by Indo-French Centre for the Promotion of Advanced Research project No. 3404-4 (Dr Pumir); and by National Science Foundation grants 0800793 (Drs Fenton and Cherry) and BES-0503336 (Dr Bodenschatz). Drs Luther and Bodenschatz acknowledge support from the Max Planck Society. This work also was supported in part by the Kavli Institute for Theoretical Physics under National Science Foundation grant PHY05-51164 and by the National Science Foundation through TeraGrid resources provided by the Pittsburgh Supercomputing Center.

Disclosures

None.

References

1. Waktare JE. Cardiology patient page: atrial fibrillation. *Circulation*. 2002;106:14–16.
2. Heart disease and stroke statistics: 2007 update. *Circulation*. 2007;115: e69–e171.
3. Nattel S, Opie LH. Controversies in atrial fibrillation. *Lancet*. 2006;367: 262–272.
4. Wijffels M, Kirchhof C, Dorland R, Allessie MA. Atrial fibrillation begets atrial fibrillation: a study in awake chronically instrumented goats. *Circulation*. 1995;92:1954–1968.
5. Ideker RE, Zhou X, Knisley SB. Correlation among fibrillation, defibrillation, and cardiac pacing. *Pacing Clin Electrophysiol*. 1995;18:512–525.
6. Koster RW, Dorian P, Chapman FW, Schmitt PW, O'Grady SG, Walker RG. A randomized trial comparing monophasic and biphasic waveform shocks for external cardioversion of atrial fibrillation. *Am Heart J*. 2004; 147:e20–e26.
7. Santini M, Pandozi C, Altamura G, Gentilucci G, Villani M, Scianaro MC, Castro A, Ammirati F, Magris B. Single shock endocavitary low energy intracardiac cardioversion of chronic atrial fibrillation. *J Interv Card Electrophysiol*. 1999;3:45–51.
8. Walcott GP, Killingsworth CR, Ideker RE. Do clinically relevant transthoracic defibrillation energies cause myocardial damage and dysfunction? *Resuscitation*. 2003;59:59–70.
9. Gillis AM, Unterberg-Buchwald C, Schmidinger H, Massimo S, Wolfe K, Kavaney DJ, Otterness MF, Hohnloser SH; GEM III AT Worldwide Investigators. Safety and efficacy of advanced atrial pacing therapies for atrial tachyarrhythmias in patients with a new implantable dual chamber cardioverter-defibrillator. *J Am Coll Cardiol*. 2002;40:1653–1659.
10. Ricci RP. Atrial tachyarrhythmia prevention and treatment by means of special pacing algorithms. *Ital Heart J*. 2005;6:200–205.
11. Israel CW, Hügl B, Unterberg C, Lawo T, Kennis I, Hettrick D, Hohnloser SH; AT500 Verification Study Investigators. Pace-termination and pacing for prevention of atrial tachyarrhythmias: results from a multicenter study with an implantable device for atrial therapy. *J Cardiovasc Electrophysiol*. 2001;12:1121–1128.
12. Ricci R, Pignalberi C, Disertori M, Capucci A, Padeletti L, Botto G, Toscano S, Miraglia F, Grammatico A, Santini M. Efficacy of a dual chamber defibrillator with atrial antitachycardia functions in treating spontaneous atrial tachyarrhythmias in patients with life-threatening ventricular tachyarrhythmias. *Eur Heart J*. 2001;3:25–32.
13. Allessie M, Kirchhof C, Scheffer GJ, Chorro F, Brugada J. Regional control of atrial fibrillation by rapid pacing in conscious dogs. *Circulation*. 1991;84: 1689–1697.
14. Pak HN, Liu YB, Hayashi H, Okuyama Y, Chen PS, Lin SF. Synchronization of ventricular fibrillation with real-time feedback pacing: implication to low-energy defibrillation. *Am J Physiol*. 2003;285: H2704–H2711.
15. Plonsey R. The nature of sources of bioelectric and biomagnetic fields. *Biophys J*. 1982;39:309–312.
16. Fast VG, Rohr S, Gillis AM, Kléber AG. Activation of cardiac tissue by extracellular electrical shocks: formation of 'secondary sources' at intercellular clefts in monolayers of cultured myocytes. *Circ Res*. 1998;82: 375–385.
17. Sharifov OF, Fast VG. Optical mapping of transmural activation induced by electrical shocks in isolated left ventricular wall wedge preparations. *J Cardiovasc Electrophysiol*. 2003;14:1215–1222.
18. Sambelashvili AT, Nikolski VP, Efimov IR. Virtual electrode theory explains pacing threshold increase caused by cardiac tissue damage. *Am J Physiol*. 2004;286:H2183–H2194.
19. Windisch H, Platzer D, Bilgici E. Quantification of shock-induced microscopic virtual electrodes assessed by subcellular resolution optical potential mapping in guinea pig papillary muscle. *J Cardiovasc Electrohysiol*. 2007; 18:1086–1094.
20. Hooks DA, Tomlinson KA, Marsden SG, LeGrice IJ, Smaill BH, Pullan AJ, Hunter PJ. Cardiac microstructure: implications for electrical propagation and defibrillation in the heart. *Circ Res*. 2002;91:331–338.
21. Trayanova N, Skouibine K. Modeling defibrillation: effects of fiber curvature. *J Electrocardiol*. 1998;31(suppl):23–29.
22. Roth BJ, Wikswo JP Jr. A bidomain model for the extracellular potential and magnetic field of cardiac tissue. *IEEE Trans Biomed Eng*. 1986;33: 467–469.
23. Plank G, Prassl A, Hofer E, Trayanova NA. Evaluating intramural virtual electrodes in the myocardial wedge preparation: simulations of experimental conditions. *Biophys J*. 2008;94:1904–1915.
24. Pumir A, Nikolski V, Hörning M, Isomura A, Agladze K, Yoshikawa K, Gilmour R, Bodenschatz E, Krinsky V. Wave emission from heterogeneities opens a way to controlling chaos in the heart. *Phys Rev Lett*. 2007;99:208101.
25. Ripplinger CM, Krinsky VI, Nikolski VP, Efimov IR. Mechanisms of unpinning and termination of ventricular tachycardia. *Am J Physiol*. 2006;291:H184–H192.
26. Fedorov VV, Lozinsky IT, Sosunov EA, Anyukhovsky EP, Rosen MR, Balke W, Efimov IR. Application of blebbistatin as an excitation-contraction uncoupler for electrophysiologic study of rat and rabbit hearts. *Heart Rhythm*. 2007;4:619–626.
27. Allessie MA, Lammers WJ, Bonke IM, Hollen J. Intra-atrial reentry as a mechanism for atrial flutter induced by acetylcholine and rapid pacing in the dog. *Circulation*. 1984;70:123–135.
28. Fenton FH, Cherry EM, Karma A, Rappel WJ. Modeling wave propagation in realistic heart geometries using the phase-field method. *Chaos*. 2005;15:013502.
29. Fox JJ, McHarg JL, Gilmour RF Jr. Ionic mechanism of electrical alternans. *Am J Physiol*. 2002;282:H516–H530.
30. Nygren A, Fiset C, Firek L, Clark JW, Lindblad DS, Clark RB, Giles WR. Mathematical model of an adult human atrial cell: the role of K+ currents in repolarization. *Circ Res*. 1998;82:63–81.
31. Spach MS, Dolber PC. Relating extracellular potentials and their derivatives to anisotropic propagation at a microscopic level in human cardiac muscle. *Circ Res*. 1986;3:356–371.
32. Kneller J, Zou R, Vigmond EJ, Wang Z, Leon LJ, Nattel S. Cholinergic atrial fibrillation in a computer model of a two-dimensional sheet of canine atrial cells with realistic ionic properties. *Circ Res*. 2002;90: e73-e87.
33. Bernus O, Wellner M, Mironov SF, Pertsov AM. Simulation of voltage-sensitive optical signals in three-dimensional slabs of cardiac tissue: application to transillumination and coaxial imaging methods. *Phys Med Biol*. 2005;50:215–229.

34. Haïssaguerre M, Hocini M, Sanders P, Sacher F, Rotter M, Takahashi Y, Rostock T, Hsu LF, Bordachar P, Reuter S, Roudaut R, Clémenty J, Jaïs P. Catheter ablation of long-lasting persistent atrial fibrillation: clinical outcome and mechanisms of subsequent arrhythmias. *J Cardiovasc Electrophysiol*. 2005;16:1138–1147.
35. Waldo A. Atrial flutter: entrainment characteristics. *J Cardiovasc Electrophysiol*. 1997;8:337–352.
36. Alt E, Schmitt C, Ammer R, Coenen M, Fotuhi P, Karch M, Blasini R. Initial experience with intracardiac atrial defibrillation in patients with chronic atrial fibrillation. *Pacing Clin Electrophysiol*. 1994;17:1067–1078.
37. Saksena S, Prakash A, Mangeon L, Varanasi S, Kolettis T, Mathew P, De Groot P, Mehra R, Krol RB. Clinical efficacy and safety of atrial defibrillation using biphasic shocks and current nonthoracotomy endocardial lead configurations. *Am J Cardiol*. 1995;76:913–921.
38. Murgatroyd FD, Slade AKB, Sopher M, Rowland E, Ward DE, Camm AJ. Efficacy and tolerability of transvenous low energy cardioversion of paroxysmal atrial fibrillation in humans. *J Am Coll Cardiol*. 1995;25:1347–1353.
39. Lévy S. Internal defibrillation: where we have been and where we should be going? *J Interv Card Electrophysiol*. 2005;13(suppl):61–66.
40. Nikolski VP, Sambelashvili AT, Krinsky VI, Efimov IR. Effects of electroporation on optically recorded transmembrane potential responses to high-intensity electrical shocks. *Am J Physiol*. 2004;286:H412–H418.
41. Steinhaus DM, Cardinal DS, Mongeon L, Musley SK, Foley L, Corrigan S. Internal defibrillation pain perception of low energy shocks. *Pacing Clin Electrophysiol*. 2002;25:1090–1093.

CLINICAL PERSPECTIVE

This study tested whether low-amplitude shocks delivered via 2 field electrodes were capable of terminating atrial fibrillation in isolated perfused canine atria. Our expectation was that the fields induced by the 2 physical electrodes would create many "virtual" electrodes that could then be used to overdrive-pace the fibrillating tissue and thereby terminate fibrillation. The observation that this method, which we call *far-field antifibrillation pacing*, converted atrial fibrillation reliably (93% success rate) with the use of field strengths that were only 13% of the energy required to cardiovert with a single shock suggests that this method may have clinical utility. Cardioversion of atrial fibrillation with the use of lower energies could reduce the pain and tissue damage associated with a large single shock and prolong the battery life of implantable devices. Further experimental studies are needed, however, to optimize the shock protocol and to determine whether far-field antifibrillation pacing is effective and safe in vivo.

SUPPLEMENTAL MATERIAL

Supplemental Figures and Figure Legends

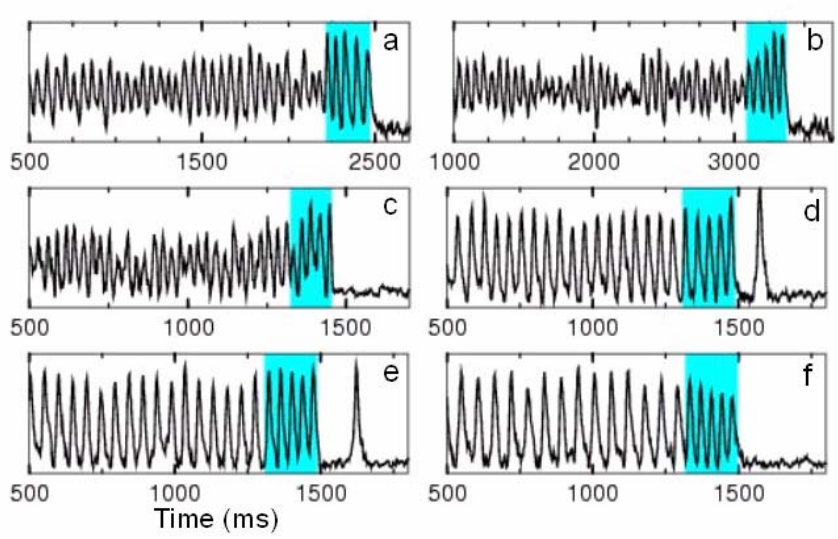

Figure I. Successful defibrillation attempts. **a-f.** Optical signals from one pixel during successful defibrillation in six different preparations. Light blue shading indicates time during applied shocks. Dominant arrhythmia periods for panels a-f are 51, 55, 30, 43, 48 and 64 ms, respectively, and the FF-AFP periods are 45, 60, 28, 40, 40 and 39 ms, respectively. Sinus rhythm resumes spontaneously after arrhythmia termination in d and f.

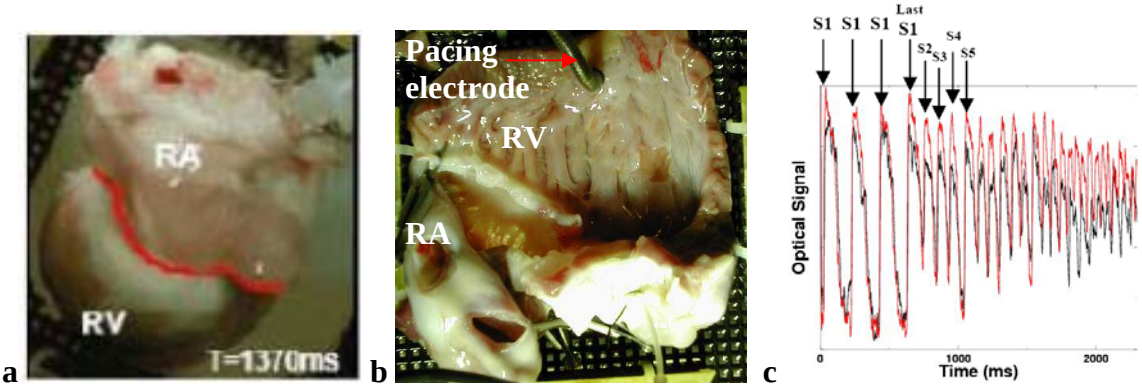

Figure II. Tissue size can support ventricular fibrillation. Although ventricular fibrillation was not observed following FF-AFP, the ventricular tissue size was large enough to support fibrillation induced directly by rapid pacing. **a.** Right ventricle and atrium preparation shown in Figures 3 and 4 of the manuscript. The ventricle is curved outward and is only partially visible from the camera angle. **b.** Similar preparation with endocardial side facing up; in this case, the ventricle is flat (bipolar pacing electrode also can be seen). **c.** Optical signal from two different sites (from supplemental movie FigS2.mov) showing a one-to-one response during pacing at a cycle length of 200 ms (S1) followed by 4 rapid pulses (S2-S5) that initiate fibrillation.

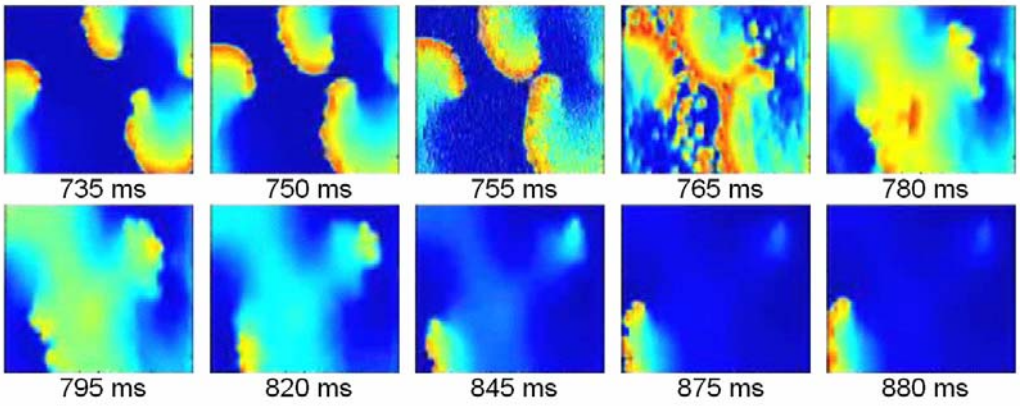

Figure III. Termination is not due to rotors being pushed to the boundaries to be annihilated. By entraining the tissue, more and more excitable gap is being entrained at the new cycle length, so termination is achieved inside the tissue. Snapshots show a simulation of FF-AFP applied to three spiral waves. One of the entraining pulses is shown in panels 3-4. The two spirals on the right are terminated by this pulse inside the tissue without the need of a boundary, while the one on the left is being pushed out further to the left. See supplemental movie FigS3.mov.

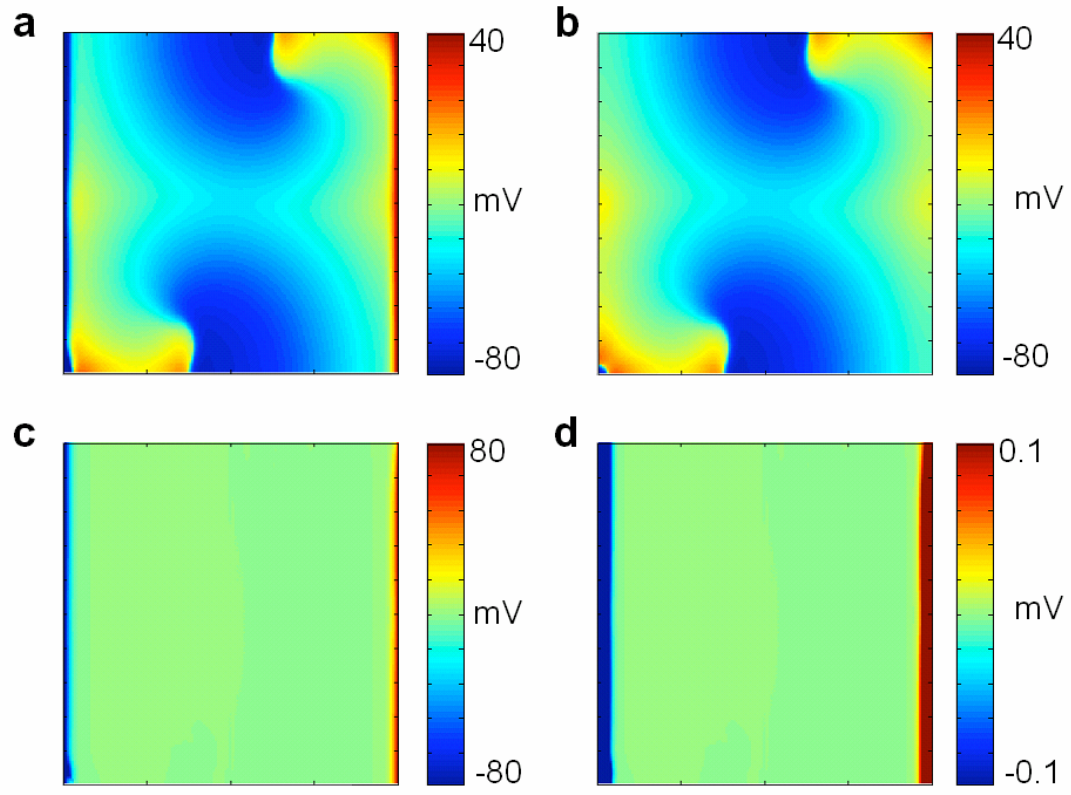

Figure IV. Effects of electric fields on dynamical electrical gradients during reentry. **a.** Reentrant waves during application of a shock (1.54 V/cm) in homogeneous tissue. **b.** Simulation from identical initial conditions without the shock. **c-d.** Difference in membrane potential between the scenarios in a and b at two different scales. Regions of hyperpolarization and depolarization greater than 0.1 mV in magnitude are produced only along the edges, so that any effects of the electric field within the tissue are negligible.

Supplemental Movie Legends

Movie I. Successful termination of AF after five field pulses of 1.4 V/cm at a cycle length of 45 ms. See Fig. 1a-d.

Movie II. Successful termination of AF after five field pulses of 1.63 V/cm at a cycle length of 40 ms. See Fig. 2a.

Movie III. Unsuccessful termination of AF after five field pulses of 0.9V/cm at a cycle length of 45 ms. See Fig. 1e-h.

Movie IV. Unsuccessful termination of AF after five field pulses of 1.40 V/cm at a cycle length of 40 ms. See Fig. 2b.

Movie V. Tissue size can support ventricular fibrillation. Although ventricular fibrillation was not observed following FF-AFP, the ventricular tissue size was large enough to support fibrillation induced directly by rapid pacing. A one-to-one response was seen during pacing at a cycle length of 200 ms followed by 4 rapid pulses that initiated fibrillation. See Data Supplement Fig. II.

Movie VI. Unsuccessful termination of AF using a single high-voltage pulse (4.67 V/cm, 5 ms duration), which fails to capture the entire tissue. See Fig. 3.

Movie VII. Successful termination of AF using a single high-voltage pulse (3.73 V/cm, 10 ms duration), which successfully captures the entire tissue. See Fig. 4.

Movie VIII. Activation site formation in an experimental preparation with two inexcitable obstacles created by cryoablation. At a low field strength of 0.18 V/cm, only the tissue edge closest to the negative electrode was activated. See Fig. 5d.

Movie IX. Activation site formation in an experimental preparation with two inexcitable obstacles created by cryoablation. Using a slightly higher field strength than for Data Supplement Movie VIII (0.28 V/cm), a slightly stronger response at the tissue edge can be seen. See Fig. 5d.

Movie X. Activation site formation in an experimental preparation with two inexcitable obstacles created by cryoablation. Using a slightly higher field strength than for Data Supplement Movie IX (0.56 V/cm), activations were initiated near the edges of the cryoablated regions closer to the positive electrode as well as at the lower edge. See Fig. 5d.

Movie XI. Activation site formation in an experimental preparation with two inexcitable obstacles created by cryoablation. Using a slightly higher field strength than for Data Supplement Movie X (0.65 V/cm), a slightly stronger response can be seen. See Fig. 5d.

Movie XII. Activation site formation in an experimental preparation with two inexcitable obstacles created by cryoablation. Using a slightly higher field strength than for Data Supplement Movie XI (0.93 V/cm), a slightly stronger response can be seen. See Fig. 5d.

Movie XIII. Simulation of virtual electrode formation and termination of reentry in tissue with multiple small conductivity discontinuities. Reentry is terminated by eight low-voltage shocks at a cycle length corresponding to the spiral wave period. See Fig. 6d.

Movie XIV. Termination is not due to rotors being pushed to the boundaries to be annihilated. By entraining the tissue, more and more excitable gap is being entrained at the new cycle length, so termination is achieved inside the tissue. FF-AFP is applied to three spiral waves. The two spirals on the right are terminated inside the tissue during the second pulse without the need of a boundary. See Data Supplement Fig. III.

Movie XV. Additional example of successful AF termination with FF-AFP using 1.6V/cm and 5 pulses.

Movie XVI. Additional example of successful AF termination with FF-AFP using 1.6V/cm and 5 pulses. The arrhythmia frequency is lower than that of Movie XV.